Development of boron liquid metal ion source for focused ion beam system

R. H. Higuchi-Rusli, K. C. Cadien,[a] J. C. Corelli, and A. J. Steckl
Center for Integrated Electronics, Rensselaer Polytechnic Institute, Troy, New York 12181

(Received 11 June 1986; accepted 19 September 1986)

Boron liquid metal ion sources (LMIS) for the recently acquired VG focused ion beam system have been developed, and $Pd_{73}B_{27}$ binary eutectic alloy was selected as the *p*-type dopant source. A lifetime of more than 120 h has been recorded and three different emitter tip radii were used to test boron ion beam stability. Microstructure examination of the $Pd_{73}B_{27}$ binary alloy proved that boron LMIS instability was caused primarily by the formation of solid precipitates due to a change in alloy stoichiometry. Auger electron spectroscopy (AES) analysis of boron beam deposited on a flat silicon substrate shows rhenium emitter erosion as well as other elements (Fe, Ni, and Cr) resulting from extractor sputtering. In this paper, greater attention is placed on the metallurgical aspects of LMIS in order to develop more reliable boron LMIS.

I. INTRODUCTION

Liquid metal ion source (LMIS) in focused-ion beam (FIB) system have emerged as a primary source for recent submicron level fabrication of IC devices.[1–3] In the FIB system, a LMIS is used as a high brightness source for a variety of purposes such as; direct write dopant source, micromachining, and photomask repair.

There are several LMIS which offer a variety of metal ion species. Of these, boron attracts considerable interest because it is the most common *p*-type dopant for submicrometer IC fabrication. To date, although there is a large body of work on LMIS,[4–8] there is a relatively little information published about the metallurgical aspects of LMIS which affect boron ion characteristics such as source lifetime and ion beam stability. The development of reliable boron LMIS requires a basic understanding of the materials problems which affect lifetime, ion beam stability, and current density. In this paper, we report on the metallurgical aspects of $Pd_{73}B_{27}$ LMIS developed for the recently acquired VG-focused ion beam system at the Center for Integrated Electronics at RPI.

II. DUAL CARBON FILAMENT LIQUID METAL ION SOURCE

Figure 1 shows the experimental setup of a dual carbon filament LMIS in the mass spectrometer chamber. The setup comprises a retractable shutter, filament, and ionizing chamber for residual gas analysis, and a series of lenses to focus the beam into the quadrupole mass spectrometer (QMS). The quadrupole mass spectrometer was calibrated with gallium LMIS before this experiment to insure accuracy of the mass spectrometer response for the PdB source. Figure 2 shows the dual carbon filament liquid metal ion source built and developed at the CIE-RPI laboratory consists of a 10 kV, 15 A three wire electrical feedthrough on a $2\frac{3}{4}$ in. CF flange with ceramic (MACOR)[19] insulator. This type of LMIS incorporated two graphite ribbon filaments instead of one[7] and has operated more than 120 h with $Pd_{73}B_{27}$ binary eutectic alloy. Two graphite ribbon filaments are more stable than a single graphite ribbon filament and provide stable liquid metal flows from the reservoir to the emitter tip. The emitter needle is anchored in the upper graphite ribbon filament and cleaning was performed in vacuum to remove oxide on the needle surface before loading with $Pd_{73}B_{27}$ alloy in the form of small lump (1–2 mm^3). After cleaning the needle, the alloy lump is immediately inserted between the two graphite ribbons at atmospheric conditions, followed by melting in vacuum at 10^{-7} Torr to wet the needle. Liquid metal passage from reservoir to the emitter tip occurs by capillary flows through a small aperture hole in the lower graphite ribbon filament.

Three different emitter radii (2.5, 5.0, and 10 μm) made of rhenium were prepared by mechanical grinding, followed by electrochemical etch (2 min) with 5N NaOH. Input heater power in the range of 50–80 W was required to melt the alloy and maintain the liquid flow to the emitter tip.

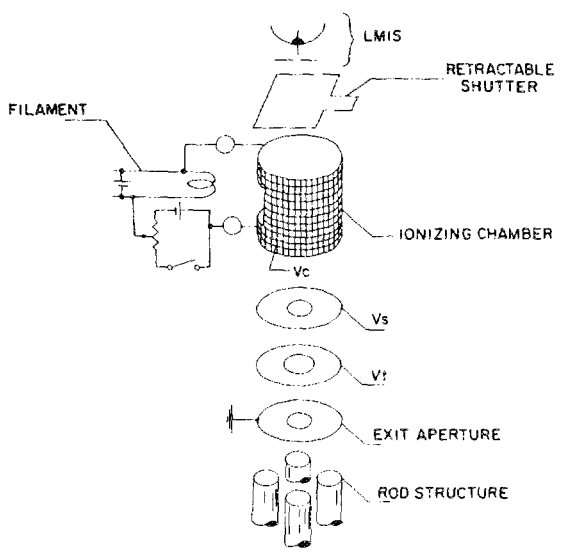

FIG. 1. Liquid metal ion source experimental setup in the QMS chamber.

 0734-211X/87/010190-05$01.00

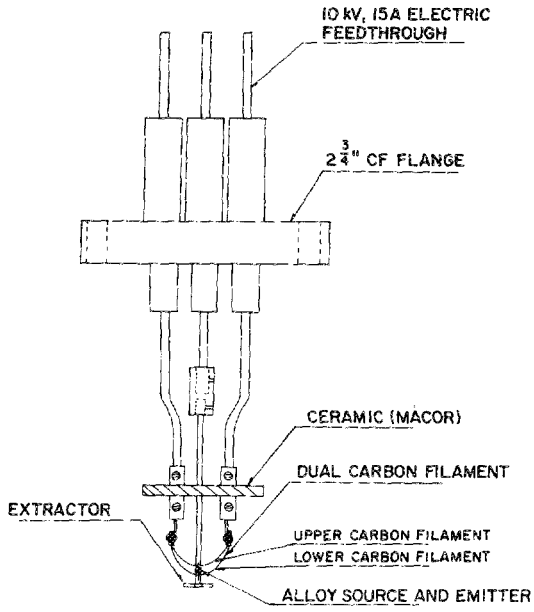

FIG. 2. Dual carbon filament liquid metal ion source.

TABLE I. Percentage abundance of various elements in beam at 3.38 μA for Pd–B alloy on Re emitter (tip radius is 2.5 μm).

Elements	Current (A)	% Abundance
$^{11}B^+$	4.1×10^{-7}	12.13
$^{10}B^+$	2.0×10^{-7}	5.91
$^{104}Pd^{++}$	1.0×10^{-7}	2.96
$^{106}Pd^{++}$	2.3×10^{-7}	6.80
$^{105}Pd^{++}$	9×10^{-8}	2.66
$^{110}Pd^{++}$	3.0×10^{-8}	0.89
$^{102}Pd^{+}$	4.0×10^{-8}	1.18
$^{104}Pd^{+}$	4.6×10^{-8}	1.36
$^{105}Pd^{+}$	4.5×10^{-7}	13.31
$^{106}Pd^{+}$	6.2×10^{-7}	18.34
$^{108}Pd^{+}$	6.0×10^{-7}	17.75
$^{110}Pd^{+}$	3.0×10^{-7}	8.87
$^{104}Pd^{11}B^{+}$	8.0×10^{-8}	2.37
$^{106}Pd^{11}B^{+}$	7.0×10^{-8}	2.07
$^{108}Pd^{11}B^{+}$	6.0×10^{-8}	1.77
$^{110}Pd^{11}B^{+}$	5.0×10^{-8}	1.48

III. RESULT AND DISCUSSION

A. $Pd_{73}B_{27}$ LMIS mass spectrum and operating characteristics

A typical mass spectrum of $Pd_{73}B_{27}$ LMIS with 2.5 μm radius emitter tip shown in Fig. 3 was obtained from the QMS with a low scanning rate of 0.5 amu/s and a total scanning width of 140 amu on the horizontal scale. The boron isotopic ratio is quite consistent with the natural boron isotopes abundance ratio. The spectrum shows doubly ionized palladium Pd^{++} which is a typical postionization of singly ionized palladium, along with the molecules of PdB^+. In Table I, are tabulated various elements detected by the QMS.

The average $^{11}B^+$ current recorded (with no attempt to focus the beam) is 0.41 μA which represents 12.13% of the total beam current recorded by QMS. From the tabulated elements in Table I, $(B/Pd)_{beam} = 24.34\%$ which is less than $(P/Pd)_{alloy}$. Figure 4 shows $^{11}B^+$ current–voltage and total extractor current–voltage characteristics of $Pd_{73}B_{27}$ alloy with emitter radius 2.5 μm. The difference is more significant at higher applied voltage, where the $^{11}B^+$ current tends to saturate. Figure 5 shows stability measurement plotted as $^{11}B^+$ current vs time for three different emitter radii. For 2.5 μm radius emitter tip (see Fig 5c), the instability is less than 4% and the $^{11}B^+$ current drift becomes almost twice as large with an increase of emitter tip radius to 5 and 10 μm [see

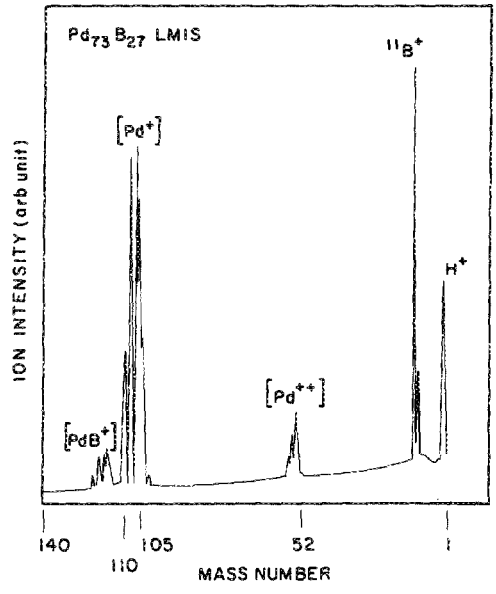

FIG. 3. Mass spectrum of $Pd_{73}B_{27}$ liquid metal ion source.

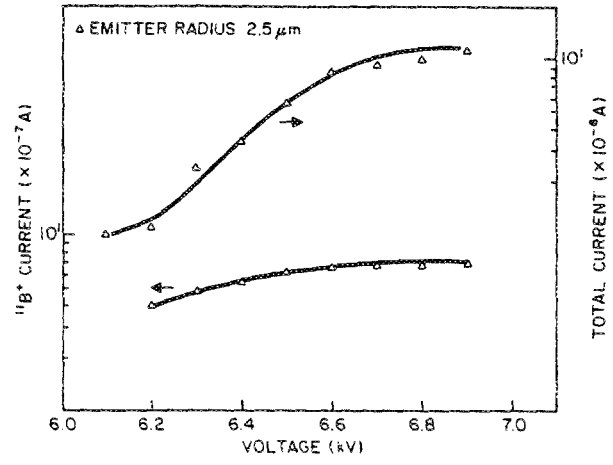

FIG. 4. Current–voltage characteristics of $Pd_{73}B_{27}$ alloy with emitter–radius 2.5 μm.

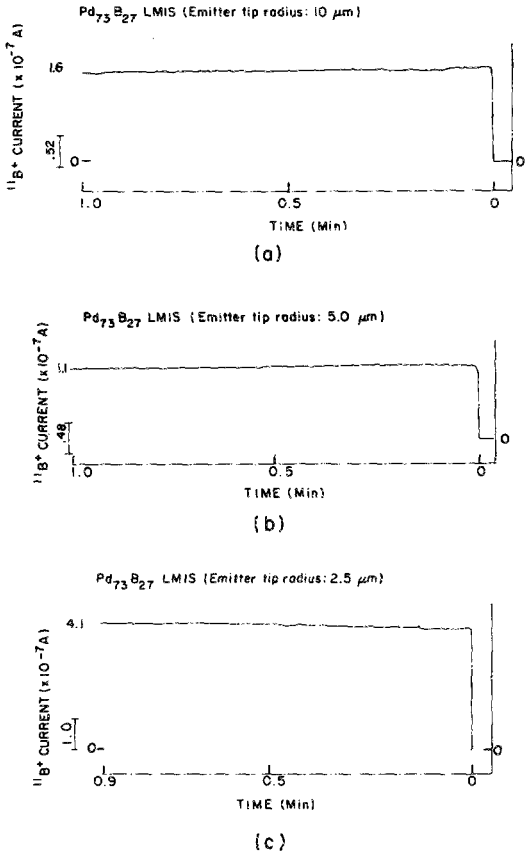

FIG. 5. Short term stability measurement of $Pd_{73}B_{27}$ liquid metal ion source with different emitter tip radius: (a) 10 μm; (b) 5.0 μm; (c) 2.5 μm.

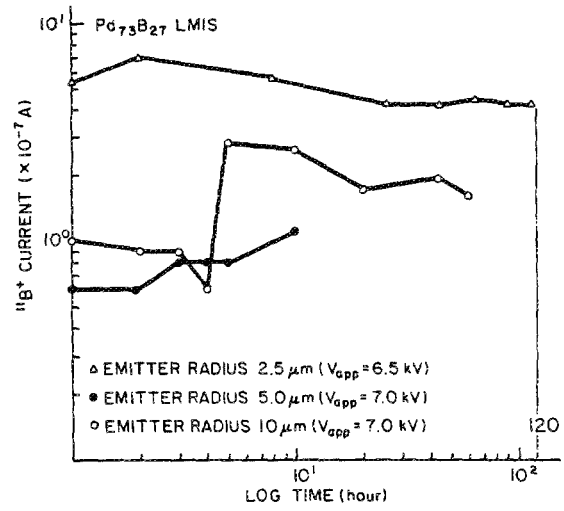

FIG. 6. Long term stability measurement of $Pd_{73}B_{27}$ liquid metal ion source with different emitter tip radii.

Figs. 5(a) and 5(b)]. The recorded $^{11}B^+$ current drift is 8.3% and 7.9% for both 5 and 10 μm emitter tips, respectively.

The $^{11}B^+$ current recorded with the same extractor condition also varies with emitter tip radius. For 5 and 10 μm emitter radius, the $^{11}B^+$ current recorded is 27% and 39% less compared to the $^{11}B^+$ current measured with 2.5 μm emitter tip.

Although short term stability measurement with different emitter radii appear to be encouraging with little $^{11}B^+$ current fluctuation, the long term stability measurement gives results which are quite different from the short term measurement. Figure 6 shows a long term stability measurement of $^{11}B^+$ current with three different emitter radii. The average $^{11}B^+$ current drift is less than 4% for 2.5 μm radius emitter tip after 120 h test run. For all three emitter tips used in this experiment, large current drift was observed during the first 10 h run. Two other sources with 5 and 10 μm radius emitter tip did not operate stably and exhibited a shorter lifetime due to mechanical failure of the graphite ribbon fastener.

B. $Pd_{73}B_{27}$ LMIS microstructures

A typical phase diagram of PdB alloy is shown in Fig. 7. The eutectic composition occurs at 24.2 at. % B and varies up to 27 at. % B.[10,11] Figure 8(a) depicts an electron micrograph of the tip of a wetted 5 μm radius rhenium emitter needle which shows visible solid precipitates of approximately 1 μm size. From the phase diagram shown in Fig. 7, it is most likely that a slight digression from a single phase eutectic composition during field evaporation shifts the single phase to a two phase region of solid and liquid. Therefore, it is conceivable that the solid precipitates occur because of a change in stoichiometry from a single phase to two phase mixture of solid and liquid. The most probable reason for the change in stoichiometry is a local concentration buildup of segregated Pd-rich alloy from Pd_3B alloy which is left behind during field evaporation. Based on the PdB phase dia-

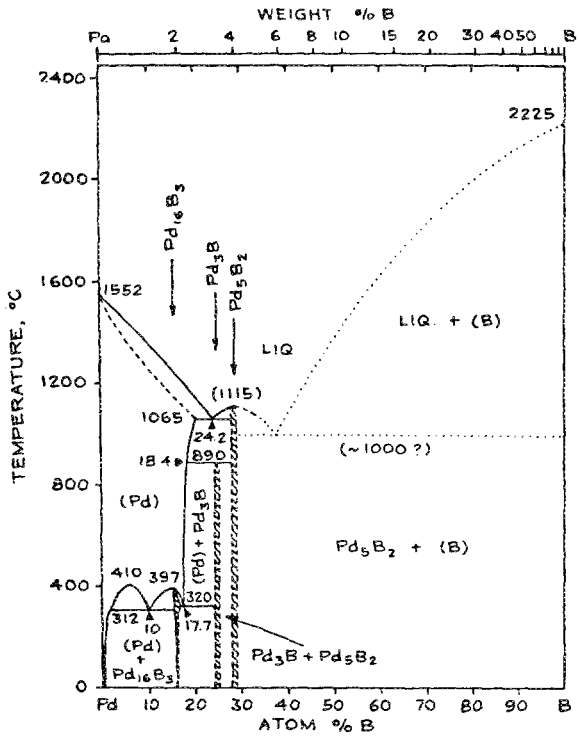

FIG. 7. B–Pd constitution phase diagram (Ref. 10).

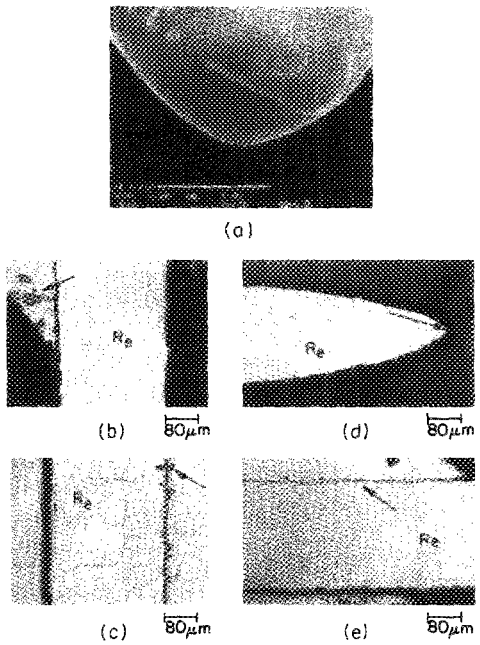

FIG. 8. Microstructures of $Pd_{73}B_{27}$ liquid metal ion source; (a) 5 μm tip by SEM; (b) metallograph of a 5 μm tip with solid precipitates in the alloy reservoir as shown by an arrow; (c) metallograph of a 5 μm emitter shows precipitate migration shown by an arrow; (d) metallograph of a 10 μm tip shows rounding off the tip as shown by an arrow; (e) metallograph of a 10 μm tip shows intermetallic precipitates at the interface of emitter tip.

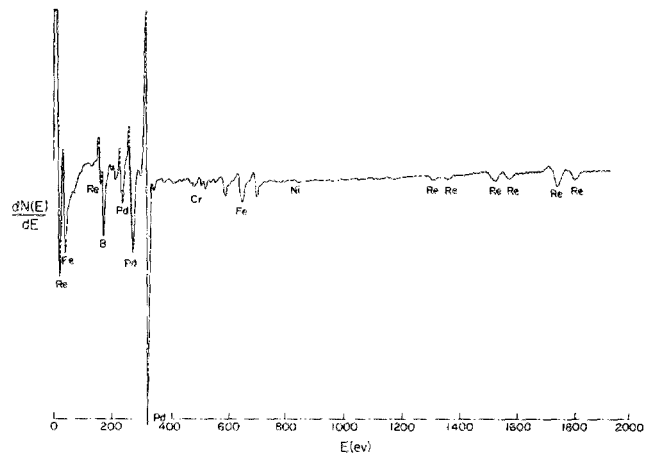

FIG. 9. Auger electron spectroscopy of a liquid metal ion source deposit on a silicon solid surface using a 10 μm emitter tip radius.

gram, it is less likely that boron will segregate from Pd_3B to form a B-rich alloy plus Pd_5B_2 because this will involve a large change in composition although the $(B/Pd)_{beam}$ is less than $(B/Pd)_{alloy}$, which means more boron is left in the liquid alloy. A second possibility to explain the change in alloy stoichiometry is the formation of intermetallic compound precipitates of $Pd_3B + Pd_5B_2$ in the liquid as more boron is left behind [see Figs. 8(a) and 8(b)] and, subsequently, the precipitates migrate along the shank to the tip apex of emitter needle as shown in Figs. 8(a) and 8(c). These solid phases eventually cause ion beam instability [see Fig. 5(b)] by impeding the flow of liquid metal to the tip apex. Consequently, the formation of intermetallic compounds of $Pd_3B + Pd_5B_2$ in the liquid produce a beam with stoichiometry low in $^{11}B^+$ specie of interest. This may be one of the reasons that the tabulated ratio of $(B/Pd)_{beam}$ in Table I is less than $(B/Pd)_{alloy}$.

Emitter tip blunting and rounding off was also observed with a 10 μm radius tip [see Fig. 8(d)] and is probably caused by the hydrostatic tension stress generated by the applied electric field. The source needle configuration can be considered to be a hemispherical tip superimposed on a cylindrical shank. For this case, the tensile stress in the shank is approximately equal to σ_N, so that the maximum shear stress in the shank τ is given by $\tau = \sigma_N/2$.[12] Therefore, although the shear stress generally is not high enough to cause catastropic fracture of the emitter tip, it is sufficient to erode the emitter tip and this is known as electric field induced erosion. Figure 9 shows Auger electron spectroscopy analysis of $Pd_{73}B_{27}$ LMIS beam deposited in 3 h on a solid silicon surface which shows rhenium and other elements. Since rhenium ions are not detected by the QMS, it is more likely that most of rhenium elements detected by AES originated from emitter tip errosion and not from rhenium in the liquid alloy. Therefore, although the boron LMIS may last more than 120 h, maintaining beam stability with clean emission free from extractor sputtering elements (Cr, Fe, and Ni) remains a difficult task in the development of boron LMIS.

An interesting feature shown in Fig. 8(e) is the presence of intermetallic precipitates, which may act as a protective layer for direct contact between liquid alloy and the needle. This may be one of the reasons that the emitter needle within the alloy reservoir remains stable and is not dissolved by the boron alloy. Liquid metal diffusion into the grain boundaries was observed due to the breakup of the protective layer [see Fig. 8(c)].

IV. CONCLUSION

$Pd_{73}B_{27}$ binary eutectic alloy is a good candidate for boron LMIS for the FIB system. This criteria stems from a lifetime test of more than 120 h. A combination of rhenium as liquid metal emitter and graphite ribbon as liquid metal heater and container, respectively, is one possible way to produce a long lifetime boron source. The cause of LMIS instability for $Pd_{73}B_{27}$ has been identified and, primarily, is due to a combination of solid precipitate formation as a result of change in alloy stoichiometry to palladium rich alloy from Pd_3B alloy, and formation of intermetallic compounds of $Pd_3B + Pd_5B_2$ in the liquid. It was also found that smaller emitter tip radius (2.5 μm) operates in a more stable condition and produces a higher current than a larger emitter tip (5, 10 μm). A single crystal rhenium emitter should be used for $Pd_{73}B_{27}$ LMIS to prevent liquid metal diffusion into the grain boundaries.

ACKNOWLEDGMENT

The authors gratefully acknowledge support of this work by the Semiconductor Research Corporation.

[a] Now at Microelectronics Technology Division of Eastman Kodak Corp., Rochester, New York 14650.

[1] P. Clampitt, K. L. Aitken, and D. K. Jefferies, J. Vac. Sci. Technol. 12, 1208 (1975).

[2]P. L. Kubena, C. Anderson, R. L. Seliger, P. Julles, and E. Stevens, J. Vac. Sci. Technol. **10**, 916 (1981).
[3]K. Gamo, T. Ukegawa, Y. Inomoto, Y. Ochiai, and S. Namba, J. Vac. Sci. Technol. **19**, 1182 (1981).
[4]T. Ishitani, K. Uemura, and H. Tamura, Jpn. J. Appl. Phys. **23**, 330 (1984).
[5]T. Ishitani, A. Shimase, and H. Tamura, Jpn. J. Appl. Phys. **21**, 277 (1982).
[6]V. Wang, J. W. Ward, and R. L. Seliger, J. Vac. Sci. Technol. **19**, 1158 (1981).
[7]P. D. Prewett, Proc. 9th Symp. on ISIAT'85, Tokyo (1985).
[8]T. Ishitani, K. Uemura, S. Hosoki, S. Takayama, and H. Tamura, J. Vac. Sci. Technol. **3**, 1365 (1984).
[9]RPI-Dual Carbon Filament Liquid Metal Ion Source (U.S. Patent Pending); R. H. Higuchi-Rusli, Ph. D. thesis, Rensselaer Polytechnic Institute, Troy, NY, 1986.
[10]W. G. Moffatt, *The Handbook of Binary Phase Diagram* (General Electric Co., New York, 1981), Vol. 1.
[11]R. P. Elliot, *Constitution of Binary Alloy* (McGraw-Hill, New York, 1965).
[12]J. E. Hren and S. Ranganathan, *Field-Ion Microscopy* (Plenum, New York, 1968), pp. 64–68.